

SLOW GROUND MOTION AND OPERATION OF LARGE COLLIDERS

V.V. PARKHOMCHUK,* V.D. SHILTSEV* and G.V. STUPAKOV

*Superconducting Super Collider Laboratory, 2550 Beckleymeade Ave.,
Dallas, TX 75237, USA***

(Received 30 July 1993; in final form 8 April 1994)

Slow ground motion with frequencies much less than characteristic frequencies of an accelerator usually has been considered as not seriously affecting machine operation because of assumed complete space and time coherence of the magnet displacements. In this paper, we analyze geophysical and numerous accelerator data on uncorrelated ground motion. We demonstrate that these data in many cases can be approximated by the “ATL law” that assumes diffusive wandering of the ground elements. An equation is derived that governs closed orbit distortion caused by random (though correlated) quadrupole displacements in a large circular accelerator. Estimates for the Superconducting Super Collider (SSC) are carried out and compared with the ability of the corrections system to maintain the orbit in the collider.

KEY WORDS: Closed orbit distortion, ground motion, accelerator alignment

1 INTRODUCTION

In an ideal accelerator with well-aligned magnetic elements, the closed orbit passes through the centers of bending magnets and quadrupoles to provide optimal conditions for the operation of the machine. Any alignment errors cause a closed orbit distortion (COD), reduce the dynamic aperture of the ring, and, in an extreme situation, make it impossible to run the machine.¹ Typically, a correction system is used to counteract the magnetic errors that build up and accumulate during the operation of the machine. In large accelerators, such as the Superconducting Super Collider (SSC), Large Hadron Collider (LHC), and HERA, and which have many hundreds of magnetic elements, one of the most important sources of magnetic errors on a long time scale is the ground motion that displaces the magnets from their original position. Similar problems associated with the ground motion arise also for linear electron-positron colliders, B-factories, and a new generation of synchrotron radiation sources.

* Guest scientist from Budker Institute of Nuclear Physics, 630090, Novosibirsk, Russia

** Operated by the Universities Research Association, Inc. for the U.S. Department of Energy under Contract No. DE-AC35-89ER40486.

Numerous measurements of ground motion at accelerators (see, for example, References 2 ÷ 10) have shown that in the frequency range above 1 Hz “cultural noise” vibrations (produced by human activity) are dominant. The amplitude of this motion usually does not exceed 0.1 — 0.2 μm . Below 1 Hz the most visible vibrations are microseismic waves (with a period of approximately 7 s and a wavelength of several tens of kilometers) with the amplitudes 0.1 — 10 μm . In Reference 12, COD in a periodic FODO lattice perturbed by a plane ground wave has been considered. It was found that considerable closed orbit response to plane wave takes place if the wavelength λ is about or less than the betatron wavelength $\lambda \leq C/\nu$, where C is the circumference of the ring and ν is the tune. Waves having the wavelength $\lambda \gg C/\nu$ perturb the beam motion in the ring only adiabatically, their response being proportional to a small factor of $(C/\nu\lambda)^2$.

In addition to microseismic noise, there exists an ambient low-frequency ground motion that is generated by local sources such as winds, temperature gradients, etc., and cannot be adequately treated as waves propagated in the ground. To study the effect of such motion one has to develop a theory that takes into account spatial correlation between displacements of two different points on the ground surface. In this paper we present our analysis of the problem.

In Section 2, a brief overview is given of the existing data on ground motion. Section 3 is devoted to the diffusive model of ground motion that is often referred to as the “ATL law”. In Section 4, we formulate an equation that relates COD with the spatial correlation function of the ground displacements. The derivation of this equation is contained in Appendix B. In Appendix A, several methods are presented that allow us to numerically simulate random displacements governed by the ATL law.

2 ANALYSIS OF DATA FROM EXISTING ACCELERATORS

In recent years, measurements of ground motion in a wide range of frequencies have been performed at several accelerator sites around the world.¹¹ Figure 1 shows the spectral density of the ground motion as a function of frequency f for different places. A distinctive feature of these spectra is that all of them rapidly grow when f goes to zero. A very rough interpolation of the spectra shown in Figure 1 in the region of low frequencies suggests a scaling law $S \approx f^{-3}$.

By definition, the integral of the spectral density over a frequency interval gives the averaged square of the displacement produced by the ground motion in this frequency range. If one uses interpolation $S \approx f^{-3}$ mentioned above, the resulting integral diverges when integrated from zero. This gives rise to an important question of how one can evaluate COD produced by the low-frequency ground motion. It is clear, however, that from the point of view of COD the divergence of the integral is not relevant to COD because, presumably, very low-frequency motion is well correlated on the ring diameter and displaces the accelerator ring as a rigid body. This kind of displacement cannot be detected as COD, because the orbit will be moving together with the magnets and diagnostic tools. Hence, for large machines, the most dangerous displacement will be uncorrelated relative shifts of the quadrupoles that produce COD proportional to square root of the number of the quads in the ring.

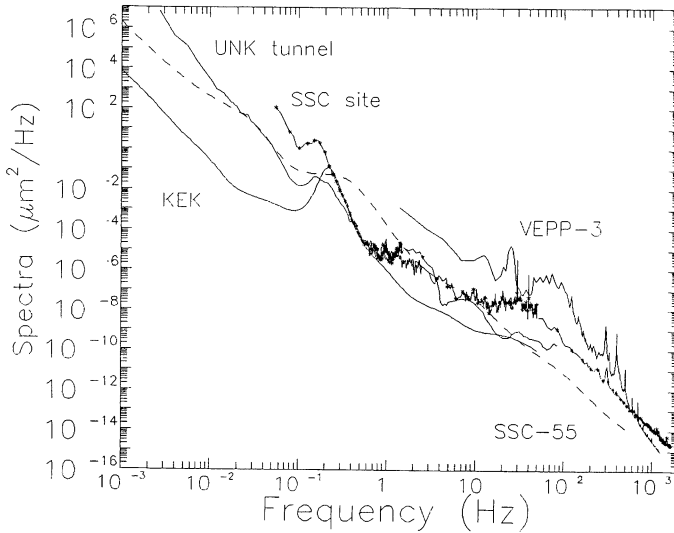


FIGURE 1: Spectra of ground motion at the SSC site,⁹ at VEPP-3 storage ring,⁶ UNK tunnel,⁵ KEK²³ and from Reference 10. All data obtained under “quiet” condition.

In addition to direct measurements of the ground motion, there are several observations of COD in existing accelerators. To compare these data for different machines, it has been proposed in Reference 13 to relate ΔX_{COD} with displacements of the quadrupoles δx assuming that the measured COD is solely due to independent displacements of the quads in the ring. For a given tune ν the equation for the δx reads: $\delta x^2 \approx \Delta X_{COD}^2 \cdot \sin^2(\pi\nu)/(4\pi\nu)$. Of course, this equation neglects a contribution to COD of the internal noise in the accelerator, so that the resulting data give an upper limit for the actual ground motion. The estimation of spectral density of the displacements thus calculated for KEK Photon Factory and HERA (electron ring), along with a spectra of COD in the Novosibirsk VEPP-3 electron storage ring and in the HERA(e) are shown in Figure 2. The dashed line in this figure represents the fit

$$S(f) = 0.03/f^2, \quad (1)$$

where $S(f)$ is measured in $\mu\text{m}^2/\text{Hz}$ and f in Hz. Empty crest mark in Figure 2 represents estimation of decade power spectral density of orbit data measured at KEK photon factory¹⁴ and corresponds to a horizontal COD of about $60 \mu\text{m}$ in 2 h; several points for HERA(e) at frequencies about 0.01 – 0.1 Hz show the results of Fourier transformation of the data from² with a maximal COD of about $200 \mu\text{m}$ in the time interval of 80 s.

Some data at even lower frequencies (corresponding to a time period of a few days) have been reported from the KEK TRISTAN storage ring. Figure 3, taken from Reference 15, shows COD in TRISTAN at 8.0 GeV. Full circles in the figure are the rms values of COD σ_1 as a function of time calculated with the use of the formula $\sigma_1^2 = N^{-1} \sum_{i=1}^N x_i^2$, where

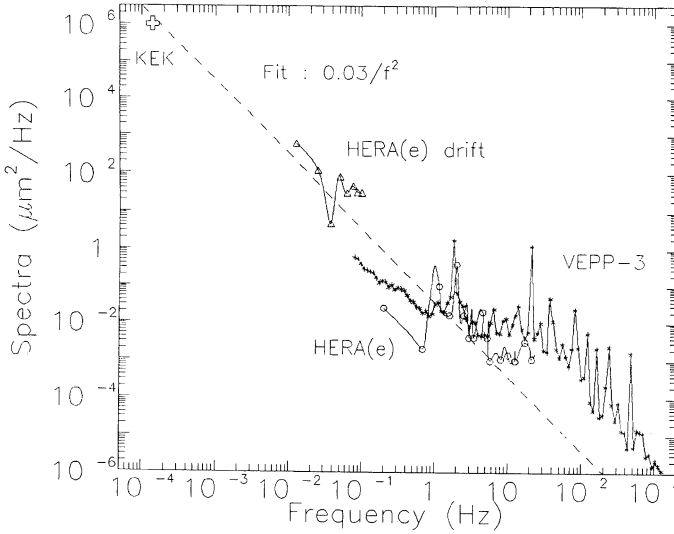


FIGURE 2: Spectra of quadrupole vibrations calculated from beam data.⁶

x_i is the measured displacement of the CO relative to the “ideal” orbit at the location of the i -th beam position monitor (BPM) and $N = 392$ is the total number of BPMs. Open circles represent the value of σ_2 , $\sigma_2^2 = N^{-1} \sum_{i=1}^N (x_i - x_{i0})^2$, where x_{i0} is the initial value of x_i during an operation cycle between two successive corrections of the orbit. Note that the horizontal COD is smaller than the vertical one. It has been observed that when σ_1 reached values larger than $100 - 200 \mu\text{m}$, the maximum beam current degraded significantly so that a correction of the orbit was needed toward the “ideal” one (sharp drops at points D, E, H, and some others in Figure 3). Using the data in Figure 3, we analyzed how CODs have been developing between the corrections. The results are summarized in Table 1, where the first column shows the time span in Figure 3, T is the duration of the time interval between the corrections of the orbit, and σ_2 is the COD accumulated in this time. We have also calculated the parameter $A = \sigma_2^2 \cdot T^{-1} \cdot C^{-1}$ ($C = 3000 \text{ m}$ is the TRISTAN circumference), the meaning of which is explained in Section 3 in connection with diffusive model of the ground motion. Note that the values of A are roughly constant, $A = (1.7 \pm 1.2) \cdot 10^{-4} \mu\text{m}^2/(\text{s} \cdot \text{m})$.

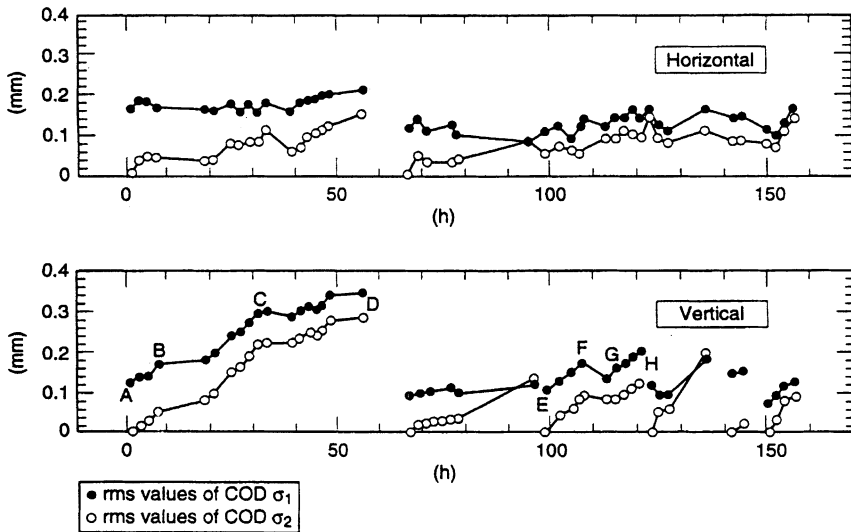
There are several interesting observations of the influence of the earth’s tides on large accelerators. Simultaneous measurements of the tide strain and the transverse beam motion in TRISTAN¹⁶ showed that the vertical beam displacement oscillates with an amplitude of approximately $200 \mu\text{m}$ in a period of 1 day, which might result from the local deformations of the tunnel under the tide forces due to geological differences along the ring.

Due to the tidal forces, the circumference of the LEP electron-positron collider varies by approximately 1 mm over the distance of 27 km.¹⁷ This minuscule effect produces detectable variations of the beam energy, which were measured using resonant depolarization technique to be $2 \cdot 10^{-5}$.

TABLE 1: Development of COD between corrections

Time interval (h)	σ_2 (μm)	T (h)	$A = \sigma_2^2 \cdot T^{-1} \cdot C^{-1}$ ($\mu\text{m}^2/(\text{s}\cdot\text{m})$)
0–50	300	50	$2 \cdot 10^{-4}$
66–96	140	30	$0.6 \cdot 10^{-4}$
97–121	140	24	$0.75 \cdot 10^{-4}$
123–135	220	12	$3.5 \cdot 10^{-4}$
150–158	120	8	$1.6 \cdot 10^{-4}$

Other important factors that influence COD are local accelerator tunnel deformations caused by temperature variations and weather conditions. According to References 7 and 16, the open air temperature variation (for example, from day to night) causes the TRISTAN tunnel deformations and results in a 0.1–0.2-mm COD in that machine. During seismic measurements at the UNK site (Protvino, Russia) an observable influence of the atmospheric pressure variation on the ground motion was detected.^{3,5} Recently this phenomenon was also measured at KEK.⁷ In Reference 18, CODs in the arcs of the SSC during a strong storm were estimated to be in the 1-mm range. Note that the beam transverse size in the arcs of the SSC is about 100 μm .



TIP-04676

FIGURE 3: Variations of the closed orbit with time at TRISTAN.¹⁵

3 DIFFUSIVE GROUND MOTION AND THE “ATL LAW”

The ATL law was originally proposed in References 5 and 3 and developed in Reference 19 to describe experimental data on relative displacement of two distant points on the ground surface. According to this law, the relative rms displacement δx of two points located at a distance L grows with time T :

$$\langle \delta x^2 \rangle = ATL, \quad (2)$$

where A is a constant that somewhat depends on the site. It was specially emphasized that such irregular diffusive motion occurs over a broad range of time intervals T (from several hours to several years) and distances L (from few meters to dozens of kilometers). One can imagine that the physical mechanisms responsible for the diffusive motion of the ground include such processes as groundwater-level variations, temperature and air-pressure fluctuations, microseismic waves, earth tides, etc., which cause random irregular displacement of ground elements due to bulk inelasticity.

We should also note that the “ATL law” describes only irregular displacements of the surface of the ground caused by “natural” sources. In addition, there always exist “artificial” disturbances (especially for new tunnels), such as heavy construction work, excavation, settling of the ground, etc., that can superimpose on the diffusive ground motion. A particular technique used for a tunnel construction may also play a role.

The ATL law is based on the results of statistical processing of raw data on ground displacements in a number of spatially distanced points. Data on long term motion of accelerators elements give an important input for the analysis because of numerous points of observation and high precision of measurements. The value of interest is *the variance* of relative displacements for all pairs of points separated by distance L after some time interval between measurements. Details of such analysis as well as discussion on the arising errors one can find, for example, in Reference 22.

Originally it was found that Equation (2) with the factor $A = (1.0 \pm 0.5) \cdot 10^{-4} \mu\text{m}^2/(\text{s} \cdot \text{m})$ is in good agreement with the data obtained from relative displacement measurements by straight wire for L varying from 1 m to 20 m and T varying from tens of seconds up to tens of hours, and with optical measurements at the UNK site for L up to 2 km and T about 2 years.⁵ Also, analysis performed in Reference 19 showed that Equation (2) is confirmed by observation of SLAC Linear Collider SLC tunnel ($L = 3$ km) displacements during 17 years,¹⁰ SLAC PEP tunnel displacements during 20 months over the circumference 2000 m,⁴ and CERN SPS quadrupoles displacements ($T = 3 - 12$ years, $C=6.6$ km).²² Figure 4 shows the dependence of $\langle \delta x^2 \rangle / T$ versus the distance L . Different curves correspond to UNK, SLC, PEP and SPS data mentioned above and to the ATL law with the coefficient $A = 10^{-4} \mu\text{m}^2/(\text{s} \cdot \text{m})$. Two empty crest marks at $L = 7$ m correspond to horizontal (upper crest) and vertical (lower crest) shifts measured by stretched wire at linear collider VLEPP facility during 15 hours.⁵ Two circles present results of measurements by 12-m and 42-m hydrostatic level systems in TRISTAN tunnel during 5 days.¹⁶ One can see that a general tendency $\delta x \propto \sqrt{T \cdot L}$ is valid within a factor of 3.

Additional confirmations of the diffusive model can be found in COD measurements on existing machines. One of them has already been demonstrated in Table 1, where the factor A has been evaluated using TRISTAN data. Also, a paper²⁰ reported about slow drifts of

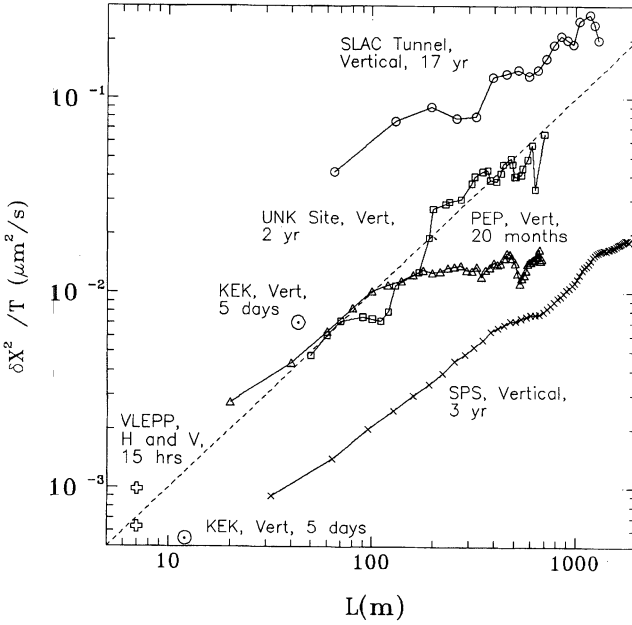


FIGURE 4: Dependence of $\langle \delta x^2 \rangle / T$ versus L .

the closed orbit that lead to 1σ beam-beam separation at electron-proton collider HERA after 10 hrs of operation, in a good agreement with expectations due to the ATL law with $A \approx 10^{-4} \mu\text{m}^2/(\text{s}\cdot\text{m})$. Recent data²¹ on more long term drifts of the COD in HERA have shown the same \sqrt{T} - type dependence but with significantly less value of the constant A .

A different look at ATL dependence is provided by an analysis of the spectrum corresponding to Equation (2). Using the relation $f \sim 1/T$, one can estimate the spectral density

$$S \sim \langle \delta x^2 \rangle / f \sim AL/f^2 \propto \text{const}/f^2. \tag{3}$$

This result is in agreement with Equation (1), derived, as already pointed out, from COD data in different accelerators, as well as with geophysical measurements of frequency spectra of the long term ground drifts at mine Sazare (Japan)²³ and Pinon-Flat observatory (CA, USA).²⁴

For computer simulations of the COD caused by diffusive ground motion, one has to be able to generate displacements that satisfy Equation (2). In Appendix A, we describe several mathematical models that allow us to simulate this kind of random displacement.

Concluding this section, we want to make two remarks.

Firstly, in spite of the fact that the value of A varies depending on the geological condition of the site (it is 7–100 times less than $10^{-4} \mu\text{m}^2/(\text{s}\cdot\text{m})$ for hard rock data^{22,24} or at significant depth^{23,22} which corresponds to 3–10 times smaller amplitude of the diffusive

motion), the T - and L - dependences of such a drift seem to be well confirmed. In further numerical examples for the SSC we will be assuming that $A = 10^{-4} \mu\text{m}^2/(\text{s}\cdot\text{m})$ as the most probable value following from the present day data.

Secondly, we have to mention that the ATL law has its own range of applicability. Though further study is needed to clarify more precisely this range, the available data shown in Figure 4 suggest that an approximate range in which the ATL law can be used expands from the distance about 10 meters to 2 kilometers and the time interval from 15 hours to 17 years.

4 CLOSED ORBIT DISTORTION IN FODO LATTICE WITH SPATIALLY CORRELATED DISPLACEMENTS OF THE QUADRUPOLES

To address the problem of COD caused by randomly displaced quadrupoles let us consider an accelerator ring having a FODO structure with $N/2$ identical FODO cells. Each cell contains one focusing and one defocusing quadrupole located at a distance l so that the circumference of the ring C is $C = Nl$. Denote the focal length of each focusing quadrupole by F_0 ; correspondingly, the focal length of a defocusing quadrupole will be $-F_0$; the value of the beta function at the location of the quads will be denoted by β_F and β_D , respectively. Let the betatron phase advance per cell be μ ; the betatron tune of the whole ring is $\nu = N\mu/4\pi$. The betatron phase advance ϕ_j for the j -th quadrupole relative to the 0-th quadrupole is equal to $\phi_j = j\mu/2$.

Assume that each quadrupole is randomly displaced in a transverse direction by the distance δ_i . Using a well-known formula for the closed orbit distortion Δx , one can easily write the expression for the mean square of Δx :

$$\langle \Delta x^2 \rangle = \frac{\beta}{4 \sin^2 \pi \nu} \sum_{i,j} \frac{\sqrt{\beta_i \beta_j}}{F_i F_j} \langle \delta_i \delta_j \rangle \cos(\phi + \phi_i - \pi \nu) \cos(\phi + \phi_j - \pi \nu), \quad (4)$$

where i and j take values $0, 1, \dots, N-1$, and β is the value of the beta function at the observation point. The angular brackets in Equation (4) stand for the averaging over the random values of δ_i .

Let us introduce the correlation function $K(n)$,

$$K(i-j) = \langle \delta_i \delta_j \rangle \quad (5)$$

which, by definition, is an even periodic function of its argument,

$$K(m) = K(-m), \quad K(m+N) = K(m). \quad (6)$$

Perform a discrete Fourier-transform of the correlation function:

$$K(n) = \frac{1}{N} \sum_{m=0}^{N/2} k_m \cos\left(\frac{2\pi nm}{N}\right) \quad (7)$$

Due to the symmetry and periodicity of $K(n)$, only $N/2 + 1$ Fourier coefficients k_m are needed to Fourier expand $K(n)$. The equation for the coefficients k_m reads

$$k_m = 2 \sum_{i=0}^{N-1} K(i) \cos\left(\frac{2\pi im}{N}\right), \quad \text{for } 0 < m < N/2,$$

$$k_0 = \sum_{i=0}^{N-1} K(i), \quad k_{N/2} = \sum_{i=0}^{N-1} (-1)^{-i} K(i). \quad (8)$$

A derivation presented in Appendix B, based on the assumption $N \gg 1$, gives the following result for $\langle \Delta x^2 \rangle$ in terms of Fourier components of the correlation function:

$$\langle \Delta x^2 \rangle = \frac{\beta N}{64 F_0^2 \sin^2 \pi \nu} \left(k_{[\nu]} (\sqrt{\beta_F} - \sqrt{\beta_D})^2 + k_{N/2-[\nu]} (\sqrt{\beta_F} + \sqrt{\beta_D})^2 \right), \quad (9)$$

where $[\nu]$ is the integer part of ν . In the derivation, we kept only terms that scale $\propto N$ and neglected terms $\sim O(1)$. Equation (9) implies that the dominant contributions to the COD come from the correlation having the wavelength equal to the betatron wave length (a fact well-known from analysis of the role of magnetic field errors in an accelerator ring¹) and FODO lattice-driven harmonics of noise where kicks from focusing and defocusing quadrupoles are adding – as in theory of closed orbit response on plane ground waves.¹²

In the limit when quadrupole displacements are fully uncorrelated, that is, $K(i-j) = \langle \delta^2 \rangle$ for $i = j$ and $K(i-j) = 0$ for $i \neq j$, from Eq. (8) it follows that $k_m = 2\langle \delta^2 \rangle$ and Eq. (9) reduces to

$$\langle \Delta x^2 \rangle = \frac{\beta N \langle \delta^2 \rangle}{16 F_0^2 \sin^2 \pi \nu} (\beta_F + \beta_D) \quad (10)$$

This result can be easily obtained directly from Equation (4) if one notes that on the right hand side nonvanishing terms have $i = j$ and substitutes the averaged value of $\cos^2(\phi_i - \pi \nu)$ by $1/2$.

In the opposite limit of a fully correlated motion of the quadrupoles (say, in the vertical direction), the ring displaces rigidly. It is evident that the closed orbit moves together with the ring so that $\Delta x = \delta$. In this limit, COD can be considered as negligibly small because it does not depend on the number of the quadrupoles N . In our approach, the correlated motion corresponds to $K(i-j) = \langle \delta^2 \rangle$ for any i and j . This gives $k_0 = N\langle \delta^2 \rangle$ and $k_m = 0$ for $m \neq 0$ which, according to Equation (9), results in $\langle \delta x^2 \rangle = 0$. The null result occurs because, as pointed out above, in the derivation of Equation (9) we neglected terms that do not scale proportionally to N .

For a Gaussian correlation function, $K(n) = \text{const} \cdot \exp(-n^2 l^2 / 2 \Delta l^2)$, having the correlation length Δl , Fourier coefficients k_m can be computed numerically. The result of the computation is shown in Figure 5 on which $\Delta x = \sqrt{\langle \Delta x^2 \rangle}$ is plotted as a function of $\Delta l/l$. Being normalized by the value of $\sqrt{\langle \Delta x^2 \rangle}$ at $\Delta l = 0$, this function rapidly falls with the increase of Δl .

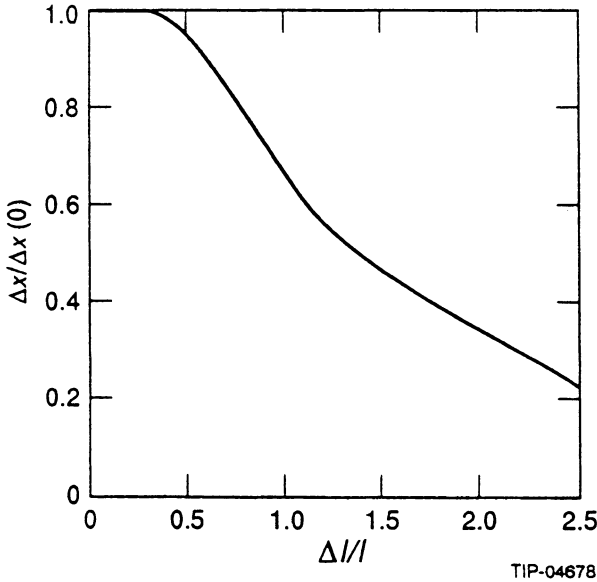


FIGURE 5: Closed orbit distortion as a function of the correlation length Δl .

Let us now apply Equation (9) to the situation when quadrupole displacements are governed by the “*ATL* law”. The “*ATL* law”, mentioned in the previous section, states that:

$$\langle (\delta_i - \delta_j)^2 \rangle = ATl |i - j| \quad (11)$$

which implies that

$$K(i - j) = D - B |i - j| \quad (12)$$

where $B = ATl/2$ and D is a constant related to a fully correlated motion of all of the quads. According to the above consideration, the constant part of $K(n)$ does not disturb the orbit so that D can be neglected. Calculations of the Fourier spectrum of the correlation function (12) with $D = 0$ yield:

$$k_m = \frac{B \cdot (1 - (-1)^m)}{\sin^2(\pi m/N)} \quad (13)$$

which gives the following equation for $\langle \Delta x^2 \rangle$:

$$\langle \Delta x^2 \rangle = \frac{\beta BN}{4F_0^2 \sin^2(\pi\nu) \sin^2(2\pi\nu/N)} \cdot \left(\beta_F + \beta_D - 2\sqrt{\beta_F \beta_D} \cos(2\pi\nu/N) \right) \quad (14)$$

TABLE 2: RMS displacement for different time intervals

T	1 s	1 min	1 h	1 day	1 month	1 yr	10 yrs	40 yrs
$\sqrt{\langle \Delta x^2 \rangle}$	3 μm	23 μm	177 μm	0.86 mm	4.7 mm	17 mm	5.2 cm	10.4 cm
$\sqrt{\langle \delta x^2 \rangle}$	0.1 μm	0.74 μm	5.7 μm	28 μm	0.15 mm	0.54 mm	1.7 mm	3.4 mm

If one uses the following identity valid for a FODO lattice, $2\sqrt{\beta_F\beta_D} = (\beta_F + \beta_D) \cos(\mu/2)$, then Equation (14) takes a simpler form

$$\langle \Delta x^2 \rangle = \frac{\beta AT C (\beta_F + \beta_D)}{8F_0^2 \sin^2(\pi\nu)} \quad (15)$$

Using Equation (15) with $A = 10^{-4} \mu\text{m}^2/(s \cdot \text{m})$, we have computed the displacement of the closed orbit at the SSC. The following SSC parameters were used: $\beta = 100 \text{ m}$, $\mu = \pi/4$, $\beta_F = 305 \text{ m}$, $\beta_D = 54 \text{ m}$, $C = 87120 \text{ m}$, $F_0 = 64 \text{ m}$, $l = 90 \text{ m}$, $\nu = 122.265$. The rms displacement of the closed orbit $\sqrt{\langle \Delta x^2 \rangle}$ is presented in Table 2 for different time intervals T , along with the rms value of the relative displacement of two neighboring quadrupoles $\sqrt{\langle \delta x^2 \rangle} = \sqrt{ATl}$.

Let us compare these results with the ability of the SSC correctors to displace the orbit in the ring. The maximum strength of a dipole corrector (there are one horizontal and one vertical corrector in each cell) is about 3 T·m,²² which corresponds to the maximum angle correction $\delta\theta_{\text{max}} = 45 \mu\text{rad}$ at 20 TeV. According to Reference 26, an allowable rms value of $\delta\theta$ should be 4–5.5 times smaller than $\delta\theta_{\text{max}}$, $\delta\theta_{\text{rms}} = 8 - 11.5 \mu\text{rad}$. It corresponds to a “local” alignment tolerance (offset of a quadrupole from the line joining its nearest neighbors) of about $\delta x = \Delta\theta_{\text{rms}} \cdot F = 520 - 720 \mu\text{m}$, which, according to Table 2, accumulates after only 1-2 yr. After this period of time one may expect that in several cells the maximum correction strength will not suffice to compensate for the accumulated misalignment. We have to emphasize here that “local” correction of the beam orbit does not return it to the original position, but instead makes it pass through the current centers of (displaced) quadrupoles. An attempt to keep the initial orbit in its original form would result in its shift relative to the center of the vacuum pipe and a substantial decrease of the dynamic aperture after only 4 months of operation.

According to Reference 26, the dominant physical constraint on the accuracy of the “global” survey at the SSC consists in the requirement that “the proton path length in the two halves of the ring (from the east campus area to the west campus area) must be equal to within 5 cm in order for collisions to take place at predicted locations”. This allows us to estimate the time T after which a mechanical realignment will be needed to compensate for the change of the perimeter $\Delta C = 5 \text{ cm}$. Using $\Delta C \approx \sqrt{ATC}/2$ one finds $T \approx 2 \text{ yr}$. After this time it will be necessary to replace quads to their “ideal” initial positions.

ACKNOWLEDGEMENTS

The authors wish to thank P. Lebedev, V. Lebedev, and A. Sery for many valuable discussions and suggestions. One of the authors, V. Shiltsev, acknowledges useful discussions with Dr. J. Rossbach (DESY) and thanks Dr. N. Yamamoto (KEK) for kindly permission to reproduce his figure of the “ATL law” surface.

APPENDIX A: MATHEMATICAL ALGORITHMS FOR THE ATL LAW

To simulate the “ATL law” in computer codes for accelerator design, one needs algorithms that produce the required space and time dependencies of the ground displacements. Several methods were suggested for these purposes.

A.1 Summation of Random Numbers

This method²⁷ is applicable to one-dimensional problems when the displacing ground points are distributed along a straight line. Consider N points located on a line so that the distance between two neighboring points is equal to l (the full length of the line array is lN). Initially, at $t = 0$, the displacement x of each point is equal to zero, $x_i^0 = 0$ for $i = 0, 1, \dots, N - 1$. A recursive procedure to calculate the displacements at time $T = k\tau$ from given displacements at the previous moment $T = (k - 1)\tau$ is the following:

$$x_i^k = x_i^{k-1} + \sqrt{A\tau l} \sum_{m=0}^i \Delta_m^k \quad (16)$$

where A is the factor in the “ATL law” and Δ_m^k are independent random Gaussian variables having the properties ,

$$\langle \Delta_m^k \rangle = 0, \langle \Delta_m^k \Delta_{m'}^{k'} \rangle = \delta_{mm'} \delta_{kk'} \quad (17)$$

where $\delta_{mm'}$ and $\delta_{kk'}$ are the Kroneker symbols. Taking the square of Equation (16) and averaging it, one easily finds that $\langle (x_i^k - x_{i+n}^k)^2 \rangle = Ak\tau nl = ATL$. If we want to model a circular machine, we have to impose a periodicity condition, $x_0^k = x_N^k$; in addition, one can subtract a constant component from x_i^k , putting $x_0^k = 0$. This will result in the following transformation:

$$x_i^k \rightarrow x_i^k - x_0^k - (x_N^k - x_0^k) \cdot \frac{i}{N} \quad (18)$$

The described algorithm is fast and gives time-dependent profiles of displacement that satisfy the “ATL law”. Figure A.1 from Reference 27 shows an example of its application for $N = 100$, $L = 3000$ m, and $T=4, 8, 12$, and 16 years. The maximum displacement is approximately 1.2 cm, which agrees well with many years of experimental observations at the SLAC 2-mile linac tunnel.

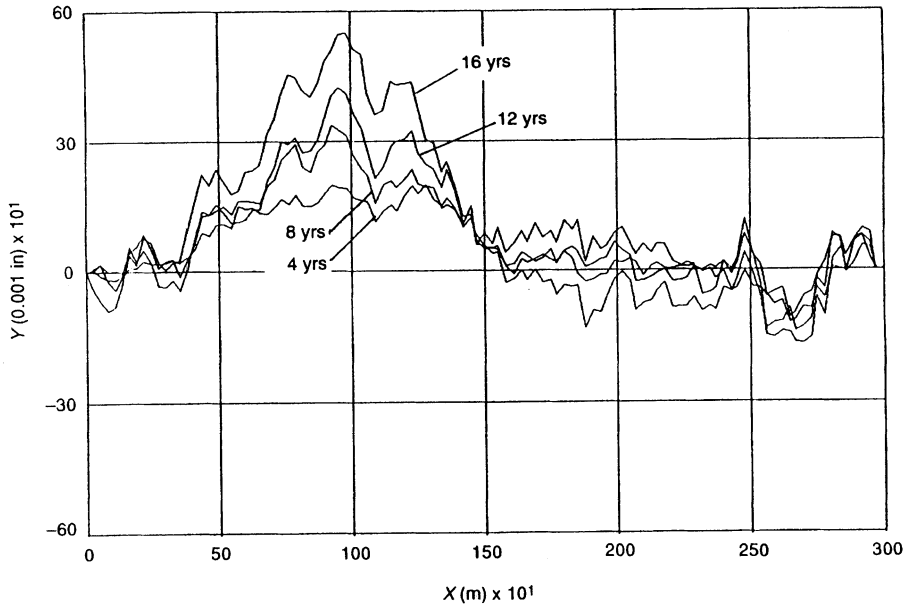


FIGURE A.1: SLAC tunnel displacements calculated according to the ATL law (from Reference 27).

A.2 Fractal Modeling of Ground Motion

This technique is based on the “fractal model” proposed in Reference 19. The model considers the ground as a set of separated blocks with different characteristic sizes R . The physical mechanism that makes blocks move is the release of its deformation energy. The model assumes that each block randomly displaces, with the rms value of the displacement being proportional to R . The rms time interval between the successive displacements is proportional to R^γ , where γ is a parameter. The model assumes also that the number of blocks $N(R)$ in a unit volume of ground having the size R depends on R as $N(R) \propto R^{-D}$. The parameters D and γ must follow the equation $\gamma = 2 - D/2$ to satisfy the ATL law.

In computer simulations described in Reference 19, the total number of blocks was about 4000. Each block was considered as a two-dimensional square; the sizes of blocks had been chosen to be $R = 1, 2, 4, 8, 16, 32, 64$ (in arbitrary units), and the parameters of the model were $D = 1.9$, $\gamma = 1.05$. The centers of the blocks were randomly distributed in the half-plane. To model the surface of the ground, 64 points were evenly distributed along the boundary of the half-space, and displacement of each point was determined as the sum of the displacements of blocks located under it. At each time step the blocks having the smallest dimension $R = 1$ were randomly displaced with displacement rms value equal to 1; blocks having $R = 2$ were displaced after 2^γ time steps randomly with rms value of the displacement equal to 2, etc. An example of the resulting profile is presented in Figure A.2.

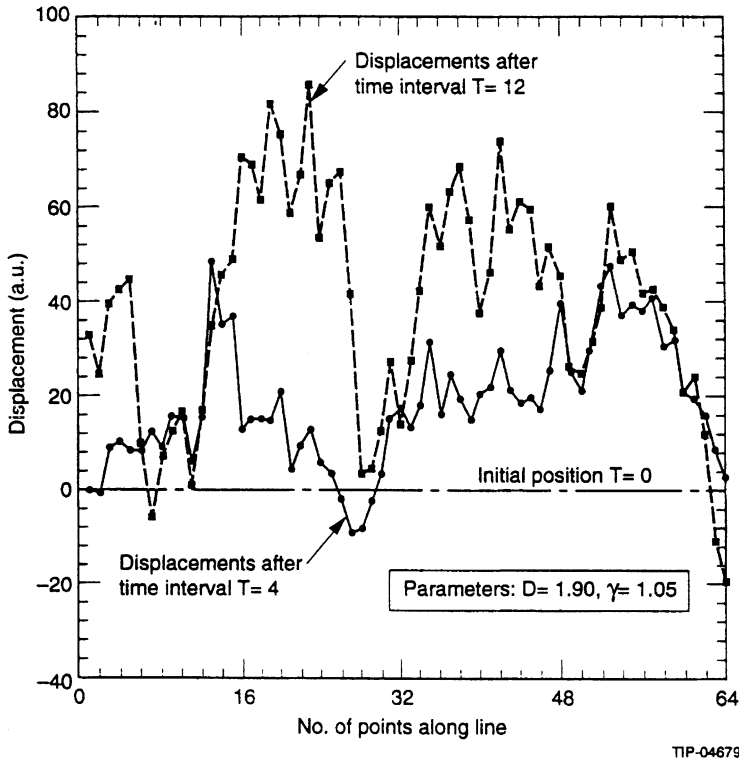


FIGURE A.2: Ground surface displacements calculated using the fractal model (from Reference 27).

A.3 Fourier Transformation of Random Functions

In Reference 28 it has been suggested to generate an n -dimensional hypersurface satisfying the “ ATL law” as a sum of random waves:

$$x(r, t) = \int d^n k |k|^{-(n+1)/2} F(k, t) \exp(-ikr) \tag{19}$$

where $F(k, t)$ is a random function satisfying the following conditions:

$$\langle F(k, t) * F(k', t) \rangle = A * t * \delta^n(k + k'), F^*(k, t) = F(-k, t) \tag{20}$$

It is easy to verify that the surface generated by $x(r, t)$ satisfies the “ ATL law” $\langle (x(r, t) - x(r + La, t))^2 \rangle \propto AtL$, where a is a unit vector. A two-dimensional surface generated using this method is presented in Figure A.3.

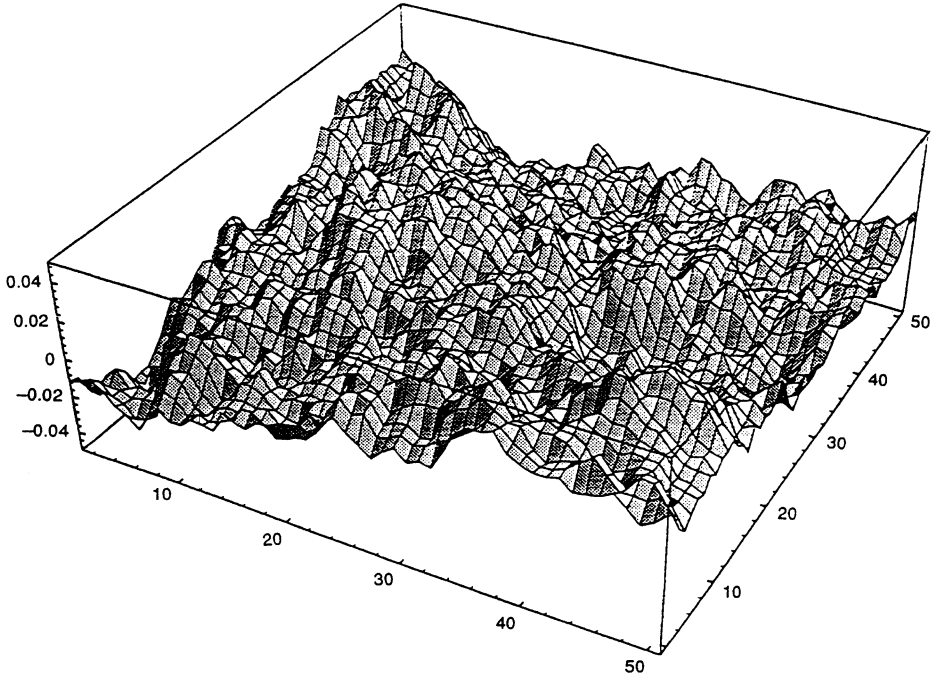


FIGURE A.3: Two-dimensional ground surface calculated by the method of Reference 27.

APPENDIX B: CALCULATION OF $\langle \Delta x^2 \rangle$

We start from Equation (4):

$$\langle x^2 \rangle = \frac{\beta}{4 \sin^2 \pi \nu} \sum_{i,j} \frac{\sqrt{\beta_i \beta_j}}{F_i F_j} \langle \delta_i \delta_j \rangle \cos(\phi + \phi_i - \pi \nu) \cos(\phi + \phi_j - \pi \nu), \quad (21)$$

First, separate Equation (21) into three sums:

$$\langle x^2 \rangle = \langle x^2 \rangle_{FF} + \langle x^2 \rangle_{DD} + \langle x^2 \rangle_{FD}, \quad (22)$$

$$\langle \Delta x^2 \rangle_{FF} = \frac{\beta \beta_F}{4 \sin^2 \pi \nu} \sum_{i,j-\text{even}} \langle \delta_i \delta_j \rangle \cos(\phi + i\mu/2 - \pi \nu) \cos(\phi + j\mu/2 - \pi \nu), \quad (23)$$

$$\langle \Delta x^2 \rangle_{DD} = \frac{\beta \beta_D}{4 \sin^2 \pi \nu} \sum_{i,j-\text{odd}} \langle \delta_i \delta_j \rangle \cos(\phi + i\mu/2 - \pi \nu) \cos(\phi + j\mu/2 - \pi \nu), \quad (24)$$

$$\langle \Delta x^2 \rangle_{DD} = \frac{\beta \sqrt{\beta_F \beta_D}}{4 \sin^2 \pi \nu} \sum_{i\text{-even}, j\text{-odd}} \langle \delta_i \delta_j \rangle \cos(\phi + i\mu/2 - \pi \nu) \cos(\phi + j\mu/2 - \pi \nu). \tag{25}$$

The first sum, $\langle \Delta x^2 \rangle_{FF}$, accounts for the focusing quadrupoles (i and j take even values); the second one, $\langle \Delta x^2 \rangle_{DD}$, gives the contribution of the defocusing quadrupoles (i and j take odd values); and the third sum, $\langle \Delta x^2 \rangle_{FD}$, results from the cross terms in which i takes even and j takes odd values.

Let's consider $\langle \Delta x^2 \rangle_{FF}$. Introducing the correlation function according to Equation (5), $K(i - j) = \langle \delta_i \delta_j \rangle$, we have

$$\langle \Delta x^2 \rangle_{FF} = \frac{\beta \beta_F}{4 \sin^2 \pi \nu} I_{FF}, \tag{26}$$

where

$$\begin{aligned} I_{FF} &= \sum_{i, j\text{-even}} K(i - j) \cos(\phi + i\mu/2 - \pi \nu) \cos(\phi + j\mu/2 - \pi \nu) = \\ &= \frac{1}{2} \sum_{i, j\text{-even}} K(i - j) [\cos(\mu(i - j)/2) + \cos(2\phi - 2\pi \nu + \mu(i + j)/2)]. \end{aligned} \tag{27}$$

For a given difference $(i - j)$, the sum $(i + j)$ takes $(N - |i - j|)/2$ values from the interval $[|i - j|, 2(N - 2) - |i - j|]$. Performing the summation over $(i + j)$, first, we find that the first term in Equation (27) has to be multiplied on $(N - |i - j|)/2$, because it does not depend on $(i + j)$. The second term oscillates as a function $(i + j)$, taking positive and negative values so in the limit $N \gg 1$ its contribution compared with a first term is $\sim O(N^{-1})$. We neglect this term in what follows:

$$I_{FF} \approx \frac{1}{4} \sum_{(i-j)} K(i - j)(N - |i - j|) \cos(\mu/2(i - j)) \tag{28}$$

where $(i - j)$ takes values from $-(N - 2)$ to $(N - 2)$. Using Fourier transformation for $K(n)$, Equation (7), one finds

$$\begin{aligned} I_{FF} &\approx \frac{1}{4N} \sum_{m=0}^{N/2} k_m \sum_n (N - |i - j|) \cos(n\mu/2) \cos(2\pi nm/N) = \\ &= \frac{\sin^2(\pi \nu)}{16N} \sum_{m=0}^{N/2} k_m \left[\sin^{-2}(2\pi(m - \nu)/N) + \sin^{-2}(2\pi(m + \nu)/N) \right]. \end{aligned} \tag{29}$$

(here we have denoted $n = i - j$).

To carry out the summation over m , we note that, in the limit $N \gg 1$, Equation 29 represents two narrow peaks around $m = [\nu]$ and $m = N/2 - [\nu]$, where $[\nu]$ denotes an integer part of ν . Assuming that k_m is smooth function of m in the vicinity of the peaks, we can approximate

$$\frac{k_m}{\sin^2(2\pi(m \pm \nu)/N)} \approx \frac{k_{j\pm}}{4\pi^2(j - \Delta\nu)^2}, \quad (30)$$

where $\Delta\nu = \nu - [\nu]$ and $j_+ = m + [\nu] - N/2$, $j_- = m - [\nu]$.

Extending summation over j from $-\infty$ to $+\infty$ one finds:

$$\sum_{-\infty}^{\infty} \frac{1}{(j - \Delta\nu)^2} = \frac{\pi^2}{\sin^2(\pi \Delta\nu)}, \quad (31)$$

and, then:

$$I_{FF} = \frac{N}{16}(k_{[\nu]} + k_{N/2-[\nu]}), \quad (32)$$

Returning to Equation (26) we have

$$\langle \Delta x^2 \rangle_{FF} = \frac{N\beta\beta_F}{64F_0^2 \sin^2 \pi\nu} (k_{[\nu]} + k_{N/2-[\nu]}) \quad (33)$$

In a similar way one can find that

$$\langle \Delta x^2 \rangle_{DD} = \frac{\beta_D}{\beta_F} \langle \Delta x^2 \rangle_{FF}, \quad (34)$$

$$\langle \Delta x^2 \rangle_{FD} = -\frac{N\beta\sqrt{\beta_f\beta_d}}{32F_0^2 \sin^2 \pi\nu} (k_{[\nu]} - k_{N/2-[\nu]}) \quad (35)$$

which for the total $\langle \Delta x^2 \rangle$ gives Equation (9).

REFERENCES

1. E.D. Courant and H.S. Snyders, "Theory of Alternating-Gradient Synchrotron", *Annals of Physics*, vol. 3 (1958) 1.
2. W. Decking, K. Floetman and J. Rossbach, "Measurements of Slow Closed Orbit Motion in Correlation with Ground Motion", *Proc. of II European Part. Accel. Conf.*, Nice, France (1990), 1449, and DESY-M-90-02, Germany (1990).
3. B.A. Baklakov, P.K. Lebedev, V.V. Parkhomchuk, A.A. Sery, V.D. Shiltsev, and A.I. Sleptsov, "Investigation of Seismic Vibrations and Relative Displacement of Linear Collider VLEPP Elements", *Proc. of 1991 IEEE Part. Acceler. Conf.*, San-Francisco, USA (1991), 3273.
4. G.E. Fischer, in *Summary and Presentation of the Workshop on Vibrational Control and Dynamic Alignment Issues at the SSC*, ed., H.J. Weaver, SSC Laboratory Special Report SSCL-SR-1185 (1992).
5. B.A. Baklakov, P.K. Lebedev, V.V. Parkhomchuk, A.A. Sery, V.D. Shiltsev, and A.I. Sleptsov, "Exploration of Correlation and Power Characteristics of Earth Surface Motion at the UNK Site", Preprint INP 91-15, Novosibirsk (1991, in Russian).

6. V.A. Lebedev, P.K. Lebedev, V.V. Parkhomchuk, and V.D. Shiltsev, "Transverse Vibrations of Electron Beam and Ground Motion Measurements at VEPP-3 Storage Ring", Preprint INP 92-39, Novosibirsk (1992), and *Proc. of 1992 Int. Part. acc. Conf.*, Dubna, Russia, Oct. 1992.
7. R. Sugahara, "Measurements of Seismic Motion and Displacement of the Floor at the TRISTAN Ring, and the Alignment Issues", KEK-Preprint 92-200, (1993).
8. V. Balakin *et al.*, "Measurements of Seismic Vibrations in CERN TT2A Tunnel for Linear Colliders Studies", CLIC-Note-191, CERN (1993).
9. V.V. Parkhomchuk, V.D. Shiltsev, and H.J. Weaver, "Measurements of Ground Motion Vibrations at the SSC", SSCL-Preprint-323, May 1993, and *Proc. of IEEE 1993 Part. Accel. Conference*, Washington, USA (1993).
10. G.E. Fischer and P. Morton, "Ground Motion Tolerances for the SSC", Preprint SSC-55 (1986).
11. V. Shiltsev, "Overview of Worldwide Seismic Measurements for Future Accelerators and Possible Choice of LC Site", *Proc. of Int. Workshop on Emittance Preservation in Linear Colliders*, KEK, Tsukuba, Japan (1993), 601.
12. J. Rossbach, "Closed-Orbit Distortions of Periodic FODO Lattices Due to Plane Ground Waves", *Particle Accelerators*, vol. 23 (1988), 121.
13. V.V. Parkhomchuk and V.D. Shiltsev, "Is Transverse Feedback Necessary for the SSC Emittance Preservation? (Vibration Noise Analysis and Feedback Parameters Optimization)", SSC Laboratory Report SSCL-622 (1993).
14. Y. Kobayashi *et al.*, "A Test of 3-GeV Operation of the Photon Factory Storage Ring", *Proc. of III European Part. Accel. Conf.*, Berlin (1992), 483.
15. H. Koiso, S. Kamada and N. Yamamoto, "Observation of Changes of the COD in TRISTAN Main Ring", *Particle Accelerators*, vol. 27 (1990), 71.
16. S. Takeda, *et al.*, "Vertical Displacement of the Base in TRISTAN", in *Proc. of 15th Int. Conf. on High Energy Accel.*, Hamburg, Germany (1992), 406.
17. *CERN Courier*, vol. 33, No.1 (1993), 4.
18. V.A. Lebedev, V.V. Parkhomchuk, V.D. Shiltsev, A.N. Skrinsky, "Suppression of Emittance Growth Caused by Mechanical Vibrations of Magnetic Elements in the Presence of Beam-Beam Effects in the SSC", INP Preprint 91-120, Novosibirsk (1991).
19. V.V. Parkhomchuk and V.D. Shiltsev, "Fractal Model of the Ground", INP Preprint 92-31, Novosibirsk (1992, in Russian).
20. R. Brinkmann and F. Willeke, "First Experience with Colliding Electron-Proton Beams in HERA", *Proc. of IEEE Part. Accel. Conf.*, Washington, DC, USA (1993).
21. R. Brinkmann, private communication.
22. V. Shiltsev, R. Stiening, "SPS Data on Tunnel Displacements and the ATL Law", SSCL-Preprint-505, SSC Lab (1993).
23. S. Takeda, *et al.*, "Slow Drift and Frequency Spectra on Ground Motion", KEK Preprint 93-61, KEK (1993), and *Proc. of III Int. Workshop on Accel. Alignment*, Annecy, CERN (1993), 225.
24. F. Wyatt, "Displacement of Surface Monuments: Horizontal Motion", *Journ. of Geophys. Research*, vol. 87, No. B2 (1982), 979.
25. Element Specification, Collider Accelerators Arc Sections, SSCL, Number E10-000027, August 1992.
26. *Site Specific Conceptual Design of the Superconducting Super Collider*, eds., J.R. Sanford and D.M. Matthews, SSC Laboratory Special Report SSCL-SR-1185 (1992).
27. V.V. Parkhomchuk, in *Summary and Presentation of the Workshop on Vibrational Control and Dynamic Alignment Issues at the SSC*, ed., H.J. Weaver, SSC Laboratory Special Report SSCL-SR-1185 (1992).
28. N. Yamamoto, in *Proc. of Int. Workshop on Emittance Preservation in Linear Colliders*, KEK, Tsukuba, Japan (1993), 693.